

DOUBLETS AND DOUBLE PEAKS: LATE-TIME [O I] $\lambda\lambda 6300, 6364$ LINE PROFILES
OF STRIPPED-ENVELOPE, CORE-COLLAPSE SUPERNOVAEDAN MILISAVLJEVIC¹, ROBERT A. FESEN¹, CHRISTOPHER L. GERARDY², ROBERT P. KIRSHNER³, PETER CHALLIS³*Submitted to the Astrophysical J. 2009 April 27; accepted 2009 December 15*

ABSTRACT

We present optical spectra of SN 2007gr, SN 2007rz, SN 2007uy, SN 2008ax, and SN 2008bo obtained in the nebular phase when line profiles can lead to information about the velocity distribution of the exploded cores. We compare these to 13 other published spectra of stripped-envelope core-collapse supernovae (Type IIb, Ib, and Ic) to investigate properties of their double-peaked [O I] $\lambda\lambda 6300, 6364$ emission. These 18 supernovae are divided into two empirical line profile types: (1) profiles showing two conspicuous emission peaks nearly symmetrically centered on either side of 6300 Å and spaced ≈ 64 Å apart, close to the wavelength separation between the [O I] $\lambda\lambda 6300, 6364$ doublet lines, and (2) profiles showing asymmetric [O I] line profiles consisting of a pronounced emission peak near 6300 Å plus one or more blueshifted emission peaks. Examination of these emission profiles, as well as comparison with profiles in the lines of [O I] $\lambda 5577$, O I $\lambda 7774$, and Mg I $\lambda 4571$, leads us to conclude that neither type of [O I] double-peaked profile is necessarily the signature of emission from front and rear faces of ejecta arranged in a toroidal disk or elongated shell geometry as previously suggested. We propose possible alternative interpretations of double-peaked emission for each profile type, test their feasibility with simple line-fitting models, and discuss their strengths and weaknesses. The underlying cause of the observed predominance of blueshifted emission peaks is unclear, but may be due to internal scattering or dust obscuration of emission from far side ejecta.

Subject headings: supernovae: general, supernovae: individual (SN 2008ax, SN 2008bo, SN 2007uy, SN 2007rz, SN 2007gr)

1. INTRODUCTION

Analyses of emission-line profiles of ejecta-tracing elements in stripped-envelope, core-collapse supernovae (CCSNe) during the “nebular phase” several months after outburst probe the chemical and kinematic properties of the metal-rich ejecta, thereby yielding clues about CCSN explosion dynamics and geometry. Particular attention has been paid to studying the line profiles of oxygen, magnesium, and calcium as these elements are among the strongest lines 100 – 200 days post-outburst (Fransson & Chevalier 1989; Filippenko 1997). Stripped-envelope SNe lacking strong H α emission (i.e., Types IIb, Ib, and Ic) can be particularly informative because details of the interior regions are not obscured by the hydrogen envelope surrounding progenitors of Type II SNe.

Late-time spectra of stripped CCSNe have shown double-peaked line profiles in [O I] $\lambda\lambda 6300, 6364$ emission to be a relatively common phenomenon, suggesting a possible unifying characteristic across types IIb, Ib, and Ic. Maeda et al. (2008) found double-peaked [O I] $\lambda\lambda 6300, 6364$ profiles in 40% of a sample of 18 stripped CCSNe, while Modjaz et al. (2008a) reported

full observing period.

Double-peaked emission-line profiles deviate from the single-peaked profile expected from a spherically symmetric source and this has been interpreted in many cases as evidence for aspherically distributed debris having a torus or disk-like geometry. Maeda et al. (2002) first predicted that double-peaked [O I] line profiles could be associated with a torus of O-rich ejecta. Mazzali et al. (2005) observed a double-peaked [O I] profile in the Type Ic broad-lined SN 2003jd, and interpreted it as emission originating from a torus of O-rich debris perpendicular to a high-velocity jet in a gamma-ray burst (GRB) model. Maeda et al. (2008) reported observing double-peaked profiles in the optical spectra of approximately 7 out of 18 CCSNe and was able to model the profiles using an aspherical, torus-like geometry of O-rich ejecta. They concluded that the observed [O I] emission could be either single- or double-peaked depending on the viewing angle being either perpendicular to or along the torus plane. Modjaz et al. (2008a) also interpreted double-peaked [O I] profiles in several CCSN spectra and found them consistent with a torus-like distribution of SN debris generated by the explosion, whereas, but not

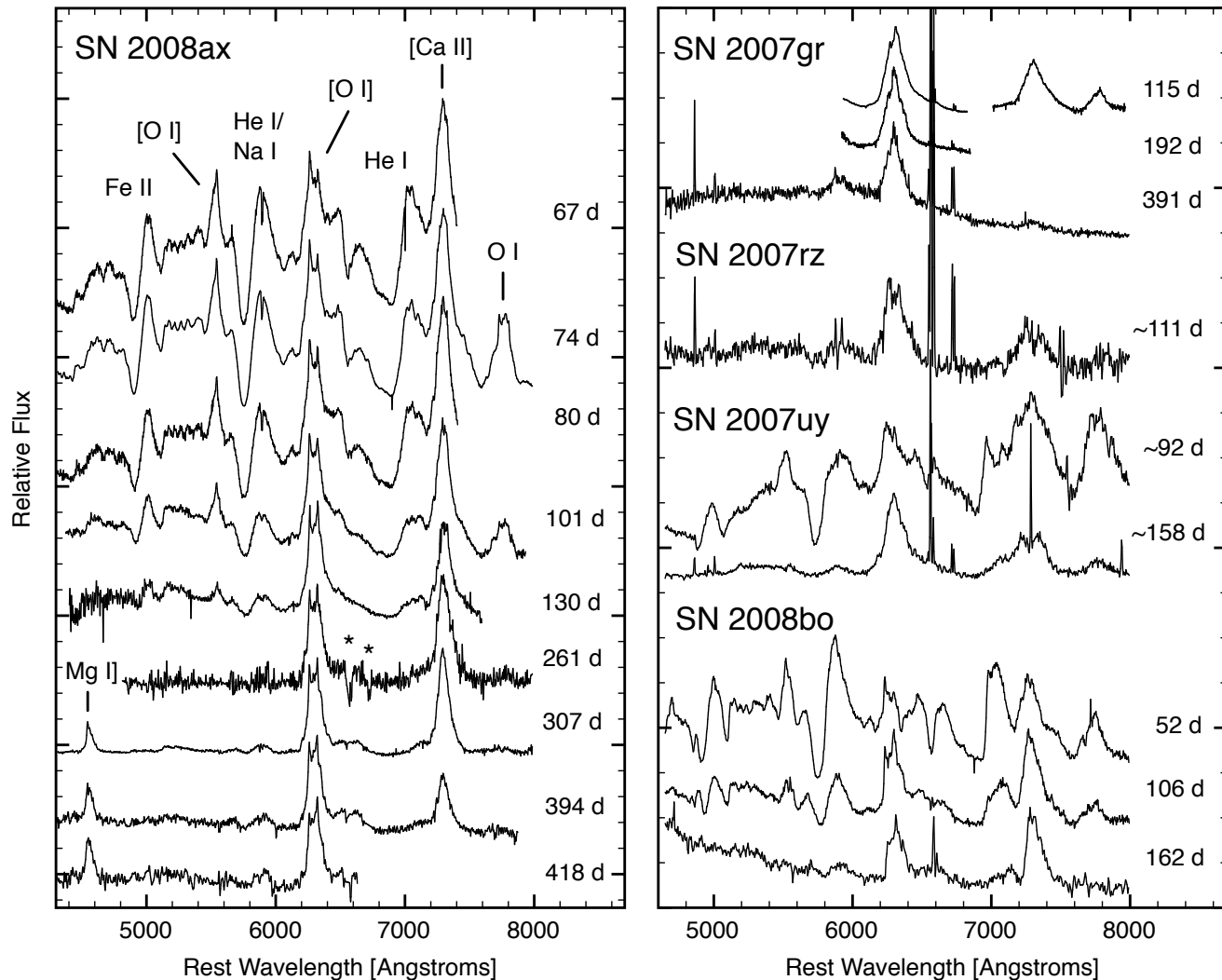


FIG. 1.— *Left panel:* optical spectra of SN 2008ax spanning its evolution into the nebular phase of emission. Asterisks (*) mark artificial features introduced during the reduction process from oversubtracted nebular lines emitted by coincident H II regions. *Right panel:* optical spectra of SN 2007gr, SN 2007rz, SN 2007uy, and SN 2008bo. See Table 1 for details of all observations.

that double-peaked [O I] line profiles are not necessarily the signature of emission from front and rear faces of O-rich ejecta arranged in a toroidal geometry as previously suggested.

2. OBSERVATIONS

Low-dispersion optical spectra were obtained with the 6.5 m MMT and the 1.5 m FLWO telescopes at Mt. Hopkins in Arizona, and the 2.4 m Hiltner telescope at the MDM Observatory on Kitt Peak, Arizona. MMT observations used the Blue Channel spectrograph (Schmidt et al. 1989) employing a $1''$ wide slit and a

or a $600 \text{ lines mm}^{-1}$ 4700 \AA blaze yielding 2 \AA resolution. The Modular Spectrograph was used in combination with the SITE 2K Echelle CCD detector with a $1.2'' \times 5'$ slit and a $600 \text{ lines mm}^{-1}$ 5000 \AA blaze grating. Resulting spectra spanned $4500 - 7500 \text{ \AA}$ with a resolution of 6 \AA . The Mark III spectrograph in combination with a SITE 1K CCD detector (‘Templeton’) was used with a $300 \text{ lines mm}^{-1}$ 6400 \AA blaze grism yielding spectra of 12 \AA resolution. Details of all observations including dates and exposure times are provided in Table 1.

All spectra were reduced and calibrated employing standard techniques in IRAF⁴ and our own IDL routines

TABLE 1
SUMMARY OF OBSERVATIONS

Supernova/ Type	Host Galaxy	Redshift ^c km s ⁻¹	Observation Date	Epoch (days)	Telescope/ Instrument	Spec. Res. (Å)	Exp. Time (s)
SN 2007gr (Ic)	NGC 1058	503	2007 Dec 21	115	MDM/CCDS	2	3000 × 3
			2008 Mar 07	192	MDM/CCDS	2	1800 × 2
			2008 Sep 22	391	MDM/Modspec	6	3000 × 3
SN 2007rz (Ic)	NGC 1590	4023	2008 Apr 01	111 ^a	MMT/Blue Channel	7 ^b	600 × 3
SN 2007uy (Ib)	NGC 2770	1874	2008 Apr 01	92 ^a	MMT/Blue Channel	7 ^b	600 × 4
			2008 June 06	158 ^a	MMT/Blue Channel	7 ^b	900
			2008 May 30	67	FLWO/FAST	10	1800
SN 2008ax (Iib)	NGC 4490	565 ^d	2008 Jun 06	74	MMT/Blue Channel	7	900
			2008 Jun 12	80	FLWO/FAST	11	1200
			2008 Jul 03	101	MDM/CCDS	11	500
			2008 Aug 01	130	MDM/Modspec	6	600
			2008 Dec 10	261	MDM/CCDS	11	2700 × 2
			2009 Jan 25	307	MMT/Blue Channel	7	1800
			2009 Apr 22 ^e	394	MDM/CCDS	11	2700 × 4
			2009 May 16	418	MDM/CCDS	11	2700
			2008 Jun 06	52	MMT/Blue Channel	7	900
			2008 Jul 30	106	MMT/Blue Channel	7	900
SN 2008bo (Iib)	NGC 6643	1484	2008 Sep 24	162	MDM/Mark III	12	2000 × 2

^a Epoch with respect to discovery date.

^b Presented spectrum smoothed with a 3 pixel boxcar function.

^c Recessional velocity inferred from narrow H α line unless otherwise noted.

^d No adjacent H α detected; NED recessional velocity of host galaxy used.

^e Presented spectrum is average of two nights of observations, 2009 April 22 and 23.

gions. When no such lines were available, host galaxy heliocentric recessional velocities were retrieved on-line from the NASA/IPAC Extragalactic Database (NED)⁵. Reported epochs are with respect to published dates of maximum optical brightness noted below, otherwise they are estimated with respect to discovery dates.

3. RESULTS

In Figure 1 we present low- to moderate-resolution late-time optical spectra of five stripped-envelope CC-SNe observed 2007–2009 at epochs spanning evolution into the nebular phase when emission is dominated by forbidden transitions. The left panel presents spectra of SN 2008ax, and the right panel spectra of SN 2007gr, SN 2007rz, SN 2007uy, and SN 2008bo. The following is a brief description of these data with particular emphasis on the emission-lines of ejecta-tracing elements oxygen, magnesium, and calcium which will be discussed in greater depth in Section 4.

3.1. SN 2008ax

SN 2008ax in NGC 4490 was discovered by Mostardi et al. (2008) on 2008 March 3 and classified spectroscopically as a Type Iib SN (Chornock et al. 2008). Extensive spectra and photometric monitoring of the SN and investigation of pre-explosion *Hubble Space Telescope* (*HST*) images show it consistent with the ex-

$\lambda\lambda 7291, 7324$ remains strong at all epochs. We interpret the relatively strong emission peaked at 4544 Å observable on days 307, 394, and 418 with Mg I] $\lambda 4571$. Oxygen emission from [O I] $\lambda 5577$ and O I $\lambda 7774$ decline in strength relative to [O I] $\lambda\lambda 6300, 6364$. Two conspicuous narrow emission peaks around 6260 Å and 6323 Å (-1800 km s⁻¹ and $+1200$ km s⁻¹, with respect to 6300 Å) are noticeable in the [O I] profile from the earliest spectrum on day 67 and persist until our last observation on day 418.

In Figure 2, we show these same spectra enlarged around emission-lines of interest to better see temporal changes in the observed features. The [O I] $\lambda 5577$ line (Figure 2, *left*) shows only a blue peak, with nearly all of the emission profile falling blueward of zero velocity. The weighted center of this emission shifts to smaller velocities with time, until day 261 when no significant [O I] $\lambda 5577$ emission is detected. On the other hand, the [O I] $\lambda\lambda 6300, 6364$ lines (*middle*) show two peaks roughly symmetric about 6300 Å. The relative strengths of the blue and red peaks change noticeably, with the blue peak stronger at early times but gradually becoming weaker at later epochs. The [Ca II] $\lambda\lambda 7291, 7324$ profile (*right*) is only modestly blueshifted and shows no change in the weighted line center over time.

Finally, we note that although SN 2008ax shares many spectral features with the SN Iib event SN 1993.I

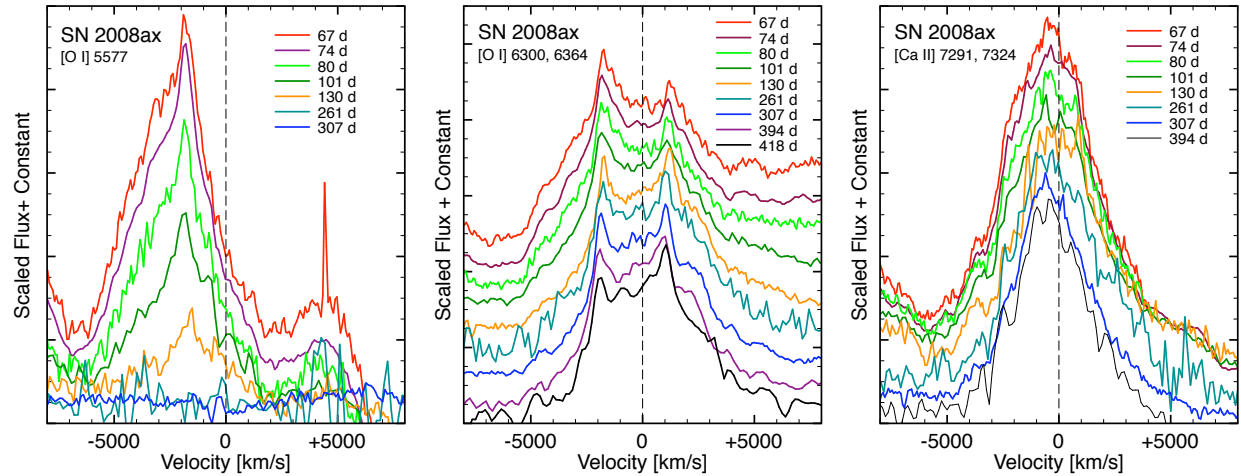


FIG. 2.— Velocity line profiles of [O I] λ 5577, [O I] λ 6300, 6364, and [Ca II] λ 7291, 7324. The dashed line marks zero velocity with respect to 5577, 6300, and 7306 Å, respectively. Time progresses from top to bottom.

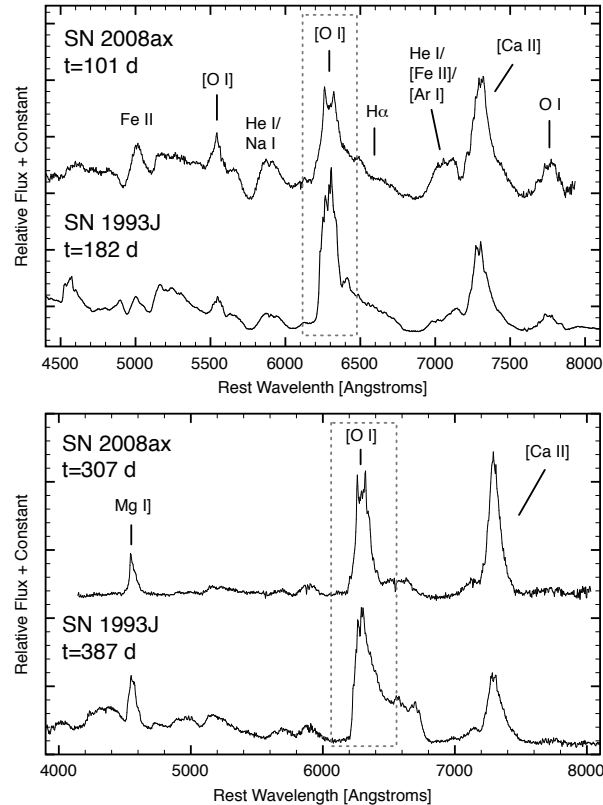


FIG. 3.— Late-time optical spectra of SN 2008ax compared to SN 1993J. Most spectral features are similar except for emission around [O I] λ 6300, 6364. The dashed box highlights SN 2008ax’s double-peaked [O I] emission and SN 1993J’s single-peaked emission. Data for SN 1993J are from Matheson et al. (2000a,b).

genitor star from a 7.0 ± 0.5 Myr cluster having a turn-off mass of $28 \pm 4 M_{\odot}$ (Crockett et al. 2008a). Extensive optical and near-infrared observations from days 5 to 415 are presented by Hunter et al. (2009).

Our moderate-resolution spectrum of SN 2007gr on day 115 (Figure 1, *right panel*) shows broad (HWZI $\gtrsim 6000$ km s $^{-1}$) [O I] λ 6300, 6364 emission strongly peaked around 6300 Å, along with [Ca II] λ 7291, 7324, and O I λ 7774 emission peaked at 7291 and 7770 Å, respectively. A minor emission peak around 6260 Å (-1900 km s $^{-1}$) is observed in the [O I] λ 6300, 6364 profile and the high signal-to-noise ratio (S/N) of the spectra ensures that this feature is real. By day 391 [O I] 6300, 6364 emission remains relatively strong and chiefly single-peaked, and the minor blueshifted peak is no longer detected.

3.3. SN 2007rz

SN 2007rz in NGC 1590 was discovered on 2007 December 12 by Parisky & Li (2007) as part of the Lick Observatory Supernova Search and classified as a Type Ic by Morrell et al. (2007). Our ~ 111 d spectrum of SN 2007rz (Figure 1, *right panel*) shows weak [O I] emission roughly symmetric about 6300 Å with two peaks at 6264 and 6330 Å (approximately -1700 and 1400 km s $^{-1}$, respectively). Broad [Ca II] λ 7291, 7324 emission centered around 7305 Å is also observed.

3.4. SN 2007uy

SN 2007uy in NGC 2770 was discovered 2007 December 31 by Y. Hirose (Nakano et al. 2008) and classified as a Type Ib by Blondin & Calkins (2008). The SN has

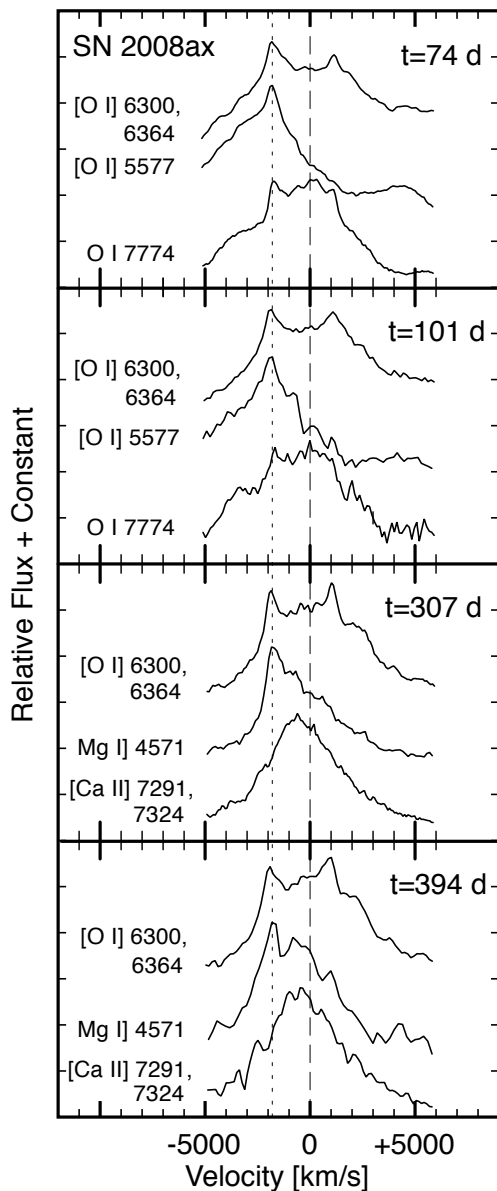


FIG. 4.— Comparing emission-line profiles of [O I] $\lambda\lambda$ 6300, 6364, [O I] λ 5577, O I λ 7774, [Ca II] $\lambda\lambda$ 7291, 7324, and Mg I λ 4571 in SN 2008ax at four epochs. The heavy dashed line marks zero velocity with respect to wavelengths 6300, 5577, 7774, 7306, and 4571 Å, respectively. The fainter dashed line highlights blueshifted peaks around -1800 km s^{-1} shared across [O I] $\lambda\lambda$ 6300, 6364, [O I] λ 5577, and Mg I λ 4571.

However, by day 158 the blueshifted peak has weakened leaving the [O I] $\lambda\lambda$ 6300, 6364 emission single-peaked and centered around 6300 \AA .

tered photometry retrieved from the SNWeb web site.⁷

Our spectra from days 52, 106, and 162 (Figure 1, *right panel*) show SN 2008bo’s entrance into the nebular phase. Blueshifted [O I] λ 5577 emission is observed on days 52 and 106 but faded and was not detected on day 162. During this time, emission from the [O I] $\lambda\lambda$ 6300, 6364 lines shows conspicuous evolution. On day 52, two peaks, one centered around 6232 \AA and another centered around 6297 \AA (approximately -3200 and 0 km s^{-1}), are seen, with the blueshifted peak stronger than the other. On day 106 the same two peaks are observed, but the blue peak is now weaker than the red one, and evidence of an additional minor peak around 6268 \AA is observed. By day 162, the blue peak continues to weaken in strength relative to emission centered around 6300 \AA . In contrast, the [Ca II] $\lambda\lambda$ 7291, 7324 lines show little relative change throughout this time period.

4. LATE-TIME [O I] EMISSION-LINE PROFILES

Our spectra of five stripped CCSNe show a variety of [O I] $\lambda\lambda$ 6300, 6364 emission profiles. SN 2008ax and SN 2007rz show double-peaked profiles that are basically symmetric about 6300 \AA . SN 2008bo and 2007uy also show double-peaked profiles but ones exhibiting strong asymmetries at early epochs. SN 2007gr, on the other hand, shows principally a single-peaked profile with a minor asymmetric blueshifted emission peak. Despite clear differences between these spectra, some trends emerge in the [O I] emission profiles when compared to other SNe.

Below, we discuss in detail the late-time emission-line profiles of SN 2008ax, which exhibit the sharpest and best-defined [O I] emission peaks compared to many other late-time CCSN spectra, and for which we have the best data set. Following this discussion, we then compare SN 2008ax’s line profiles against other SNe presented in this paper along with others taken from the literature.

4.1. SN 2008ax’s O, Ca, and Mg Emission-line Profiles

In Figure 4, we show SN 2008ax’s [O I] $\lambda\lambda$ 6300, 6364 line profile plotted in velocity space relative to other emission-lines at four epochs. The top two panels show line profiles for the three neutral oxygen lines [O I] $\lambda\lambda$ 6300, 6364, [O I] λ 5577, and O I λ 7774 from spectra obtained on days 74 and 101. Both the [O I] λ 5577 and [O I] $\lambda\lambda$ 6300, 6364 profiles show common blueshifted peaks around -1900 km s^{-1} , highlighted in this figure with the light dashed line. The O I λ 7774 profile appears square-topped with evidence for a fairly abrupt rise in emission strength close to the velocity of the [O I] λ 5577 peak and blue [O I] $\lambda\lambda$ 6300, 6364 peak.

The bottom two panels show line profiles for days 307 and 394. Emission observed at these later times should

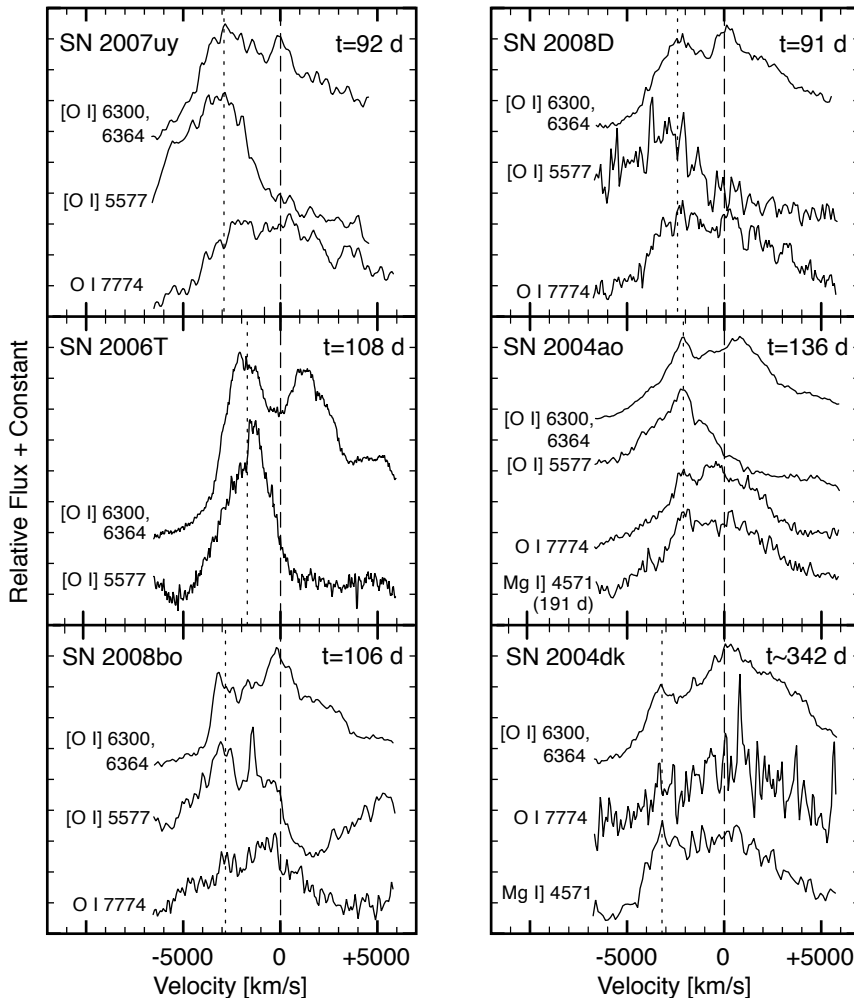


FIG. 5.— Common blueshifted peaks in the emission-line profiles of ejecta tracing elements observed in SNe at nebular epochs of optical evolution. The heavy dashed line marks zero velocity with respect to 4571, 5577, 6300, and 7774 Å in the rest frame of the SNe, while the fainter line highlights conspicuous emission peaks common across profiles. Data for SN 1993J are from Matheson et al. (2000a) and Matheson et al. (2000b), SN 2004ao, SN 2004dk, and SN 2006T from Modjaz et al. (2008a), and SN 2008D from Modjaz et al. (2008b).

epoch and the blueshifted peak of the [O I] λ 5577 profile of the two earlier epochs. Though of poorer S/N, our day 394 spectrum shows the same blueshifted peak in the Mg I] 4571 line, with possible additional emission around zero velocity. The profile of [Ca II] λ 7291, 7324 shows a slightly blueshifted, broad distribution that remains relatively unchanged at all epochs (see also Figure 2).

In summary, the emission-line profiles of ejecta tracing elements oxygen, calcium, and magnesium in the late-time spectra of SN 2008ax exhibit quite different line profiles. [O I] λ 6300, 6364 shows an unmistakable double-peaked profile at all epochs observed. In sharp contrast, the [O I] λ 5577 profile shows a prominent single-peaked

two of the four other SNe we observed (Table 1, Figure 1), along with four additional CCSNe taken from the literature. This sample is comprised of SN 2004ao (Modjaz et al. 2008a), SN 2004dk (Modjaz et al. 2008a), SN 2006T (Modjaz et al. 2008a), SN 2007uy, SN 2008D (Modjaz et al. 2008b), and SN 2008bo. Selection of these six SNe was based upon the presence of double-peaked [O I] λ 6300, 6364 line profiles and the availability of high quality late-time [O I] λ 5577, O I 7774, and Mg I] 4571 line profile data.

Figure 5 shows the emission-line profiles of these six SNe. Multiple epochs are shown for SN 2004ao because the [O I] λ 5577 and Mg I] 4571 lines are seen at dif-

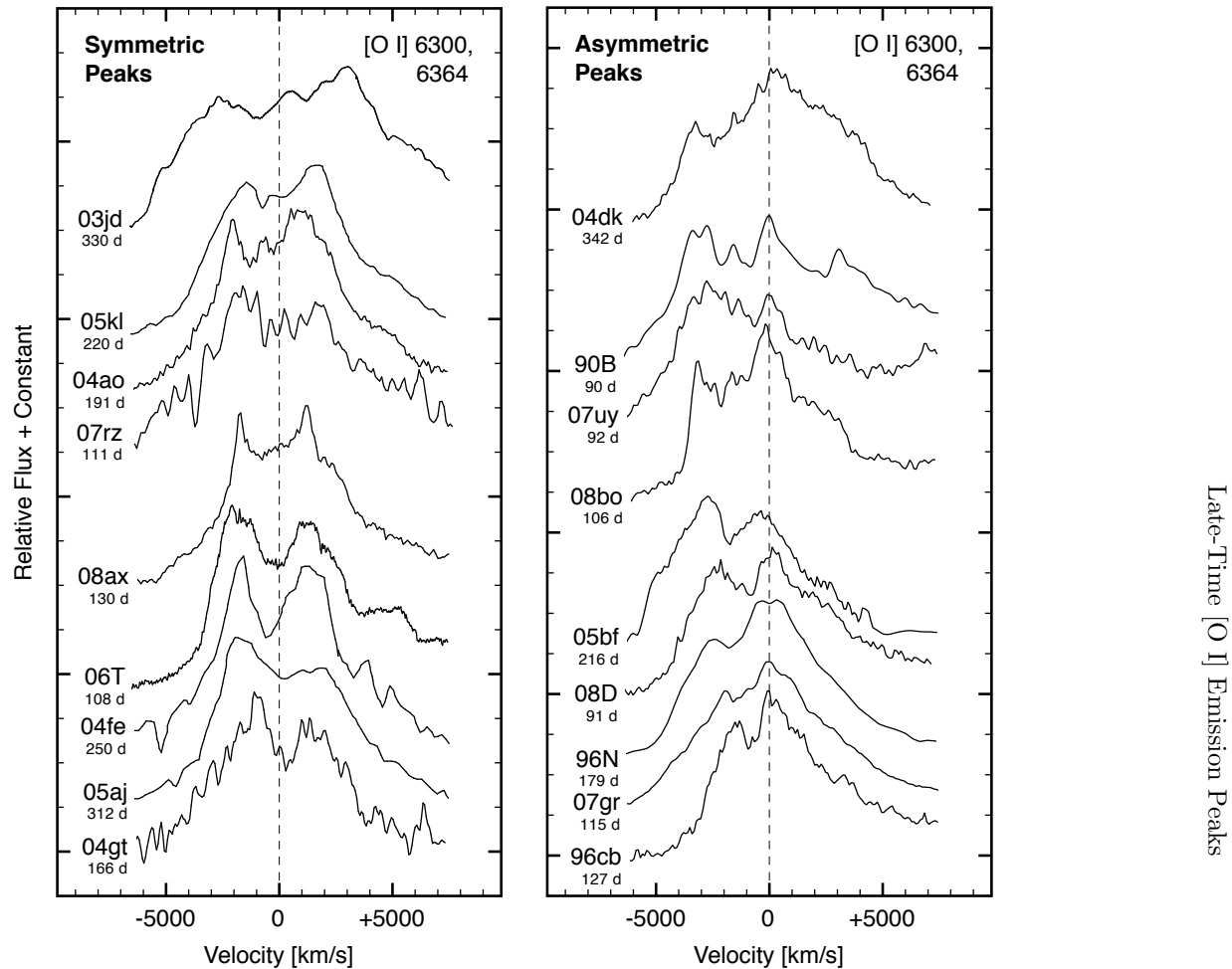


FIG. 6.— Classifying [O I] $\lambda\lambda 6300, 6364$ emission-line profiles of CCSNe at nebular epochs of optical evolution. Velocities are with respect to 6300 \AA (*dashed line*) in the rest frame of the SNe. Epochs of the observations are immediately below abbreviated supernova IDs. *Left panel*: emission-line profiles approximately symmetric about zero velocity. *Right panel*: asymmetric emission-line profiles skewed toward blueshifted velocities with one emission peak near zero velocity.

closely matching the blueshifted peak in the [O I] $\lambda\lambda 6300, 6364$ line profiles.

Also like SN 2008ax, the O I $\lambda 7774$ and Mg I $\lambda 4571$ lines of these SNe exhibit profiles noticeably different from [O I] $\lambda 5577$. Most clear is that redshifted emission is not as strong as blueshifted emission in both lines, and both O I $\lambda 7774$ and Mg I $\lambda 4571$ lines sometimes show evidence of blueshifted emission peaks at velocities matching the blueshifted peaks of the [O I] $\lambda\lambda 6300, 6364$ lines (SN 2008bo, 2008D, 2004ao, 2004dk). Additional peaks, when observed, are near zero velocity.

A recent independent survey of [O I] $\lambda\lambda 6300, 6364$ line profiles exhibited in the optical spectra of Ib/c CCSNe by Taubenberger et al. (2009) provides additional examples

on day 112.

A caveat to the trends noted above is a possible uncertainty in identifying the emission feature near 5500 \AA with [O I] $\lambda 5577$. For example, early analysis of blueshifted emission around 5500 \AA in SN 1993J was identified as [O I] $\lambda 5577$ (Spyromilio 1994; Filippenko et al. 1994; Wang & Hu 1994), but later analysis appeared to favor [O I] $\lambda 5577$ emission blended with [Fe II] $\lambda 5536$ and [Co II] $\lambda 5526$, the combination of which falsely gave the impression of blueshifted emission (Houck & Fransson 1996). However, because of the correspondence between the blueshifted peaks in the Mg I $\lambda 4571$, [O I] $\lambda 5577$, and [O I] $\lambda\lambda 6300, 6364$ lines, [O I] $\lambda 5577$

TABLE 2
REFERENCES FOR FIGURES 6 AND 7

Supernova/ Type	Host Galaxy	Observation Date	Optical Max Date	Epoch (days)	Spec. Res. (Å)	Sources/ Notes
SN 1990B (Ic)	NGC 4568	1990 Apr 18	1990 Jan 19	90	10 ^a	1 ^b
SN 1993J (IIb)	NGC 3031	1993 Sep 25	1993 Mar 27	182	7	2 ^c
SN 1996cb (IIb)	NGC 3510	1997 May 11	1997 Jan 04	127	7	3 ^b
SN 1996N (Ib)	NGC 1398	1996 Sep 07	...	179 ^d	...	4 ^d
SN 2003jd (Ic-BL)	MCG-01-59-21	2004 Sep 12	2003 Nov 01	330	5	6 ^d
SN 2004ao (Ib)	UGC 10862	2004 Sep 14	2004 Mar 07	191	10	7
SN 2004dk (Ib)	NGC 6118	2005 Jul 09	...	342 ^e	10	7
SN 2004fe (Ic)	NGC 132	2005 Jul 06	...	250 ^e	10	8 ^d
SN 2004gt (Ic)	NGC 4038	2005 Jun 09	2004 Dec 24	166	10	7
SN 2005aj (Ic)	UGC 02411	2005 Dec 27	...	312 ^e	10 ^f	8 ^d
SN 2005bf (Ib)	MCG+00-27-5	2005 Dec 11	2005 May 08	216	5 ^f	7
SN 2005kl (Ic)	NGC 4369	2006 Jun 30	...	220 ^e	10	8 ^d
SN 2006T (IIb)	NGC 3054	2006 Jun 03	2006 Feb 14	108	5	7
SN 2008D (Ib)	NGC 2770	2008 Apr 28	2008 Jan 28	91	5	9
SN 2007gr (Ic)	NGC 1058	2007 Dec 21	2007 Aug 28	115	2	10
SN 2007rz (Ic)	NGC 1590	2008 Apr 01	...	111 ^e	7 ^f	11
SN 2007uy (Ib)	NGC 2770	2008 Apr 01	...	92 ^e	7 ^f	12
SN 2008ax (IIb)	NGC 4490	2008 Jun 06	2008 Mar 24	74	7	13
SN 2008bo (IIb)	NGC 6643	2008 Jul 30	2008 Apr 15	106	7	14

REFERENCES. — (1) Clocchiatti et al. 2001 (2) Matheson et al. 2000a, Matheson et al. 2000b (3) Matheson et al. 2001, Qiu et al. 1999 (4) Sollerman et al. 1998 (5) Leonard et al. 2002, Mazzali et al. 2002 (6) Mazzali et al. 2007, Mazzali et al. 2005, Valenti et al. 2008b (7) Modjaz et al. 2008a (8) Maeda et al. 2008 (9) Modjaz et al. 2008b (10) Valenti et al. 2008a (11) Parisky & Li 2007, Morrell et al. 2007 (12) Blondin & Calkins 2008, Nakano et al. 2008 (13) Pastorello et al. 2008 (14) Nissinen & Oksanen 2008.

Note: Spectra presented in this paper have been grouped separately on the bottom.

^a Estimated from spectra using narrow H α line.

^b Downloaded from SUSPECT at <http://bruford.nhn.ou.edu/~suspect/index1.html>.

^c Downloaded from <http://www.noao.edu/noao/staff/matheson/spectra.html>.

^d Digitally traced from published spectra.

^e Epoch with respect to discovery date.

^f Presented spectra have been smoothed with a 3 pixel box car function.

the sources, observing details, and estimated epochs of all spectra. These 18 objects have been divided into two main types: nine profiles that exhibit two prominent [O I] emission peaks positioned approximately symmetrically about 6300 Å (*left panel*), and nine asymmetric profiles with one peak lying near 6300 Å and additional peaks at blueshifted velocities (*right panel*).

4.4. Symmetric [O I] Profiles

The nine [O I] $\lambda\lambda$ 6300, 6364 emission-line profiles shown in the left panel of Figure 6 share the property of exhibiting two conspicuous emission peaks positioned roughly on either side of 6300 Å. The velocity of the blueshifted emission peak ranges from ≈ -1000 to -2600 km s⁻¹ assuming it to be due to the [O I] λ 6300 line. While the peaks can be narrow as in the case of 08ax or broad as in 03jd, the presence of these two emissions peaks dominates the overall appearance of the [O I] line profiles.

a deep central trough between peaks with no obvious central emission peak (*left panel, bottom*).

Although the relative strengths of the blueshifted and redshifted peaks vary across these subgroups, in most cases the spacing between the two peaks is close to 3000 km s⁻¹ (i.e., ≈ 64 Å). The two lines of the [O I] $\lambda\lambda$ 6300, 6364 doublet (more precisely at 6300.30 and 6363.78 Å) are suspiciously close to this separation. We measured the center of the emission peaks for the profiles and found separations between 61 – 65 Å in eight of nine symmetric profiles.

The high incidence of a separation around 64 Å between emission peaks is illustrated in Figure 7, which is a montage of the eight symmetric peak profiles sharing this ≈ 64 Å separation. The exception to this group and not shown in the figure is 03jd, which shows a separation close to twice this value. SN 2004gt also appears as an exception in the relatively noisy spectrum presented here, but the much cleaner day 160 spectrum presented

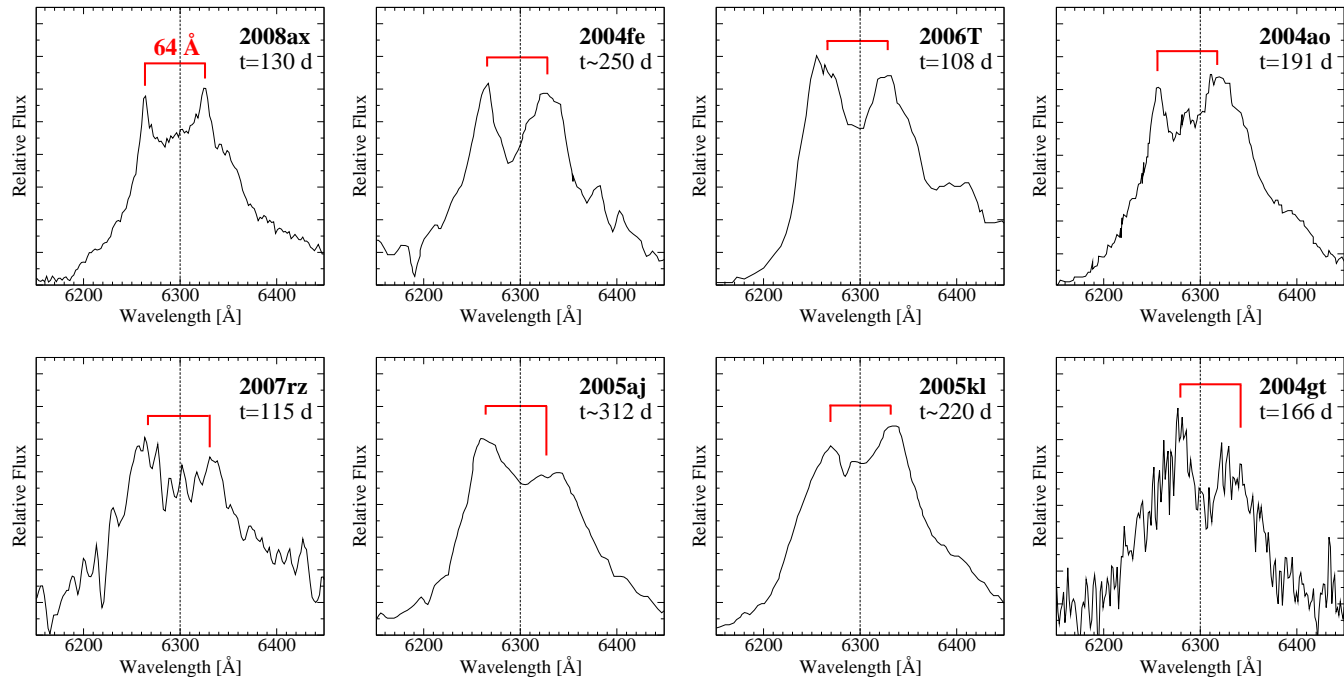


FIG. 7.— Eight of the nine late-time [O I] $\lambda\lambda 6300, 6364$ emission-line profiles showing symmetric double peaks from Figure 6. Separations of 64 \AA (marked in red) between emission peaks are common.

post-outburst. Though likely originating from different physical conditions, [O I] $6300:6364$ flux ratios around 2 and smaller are also routinely observed in novae at similar times (Williams 1994). Deviations from the 3:1 nebular value are attributed to optically thick line emission with $\tau \gtrsim 1$ (see Li & McCray 1992 and Williams 1994). We investigate other possible interpretations of these non-nebular ratios in Section 5.

4.5. Asymmetric [O I] Profiles

The nine [O I] $\lambda\lambda 6300, 6364$ emission-line profiles shown in the right panel of Figure 6 exhibit two or more emission peaks, where one peak is located close to 6300 \AA , and the other(s) blueshifted with respect to 6300 \AA producing an asymmetrical-looking line profile. As was done for the symmetric profile SN, we subdivided these asymmetric profiles into three groups. SN 2004dk, showing a relatively broad [O I] profile, forms the top grouping, while SN showing emission-line profiles that are multi-peaked or double-peaked form the middle and bottom groupings, respectively.

Much like that found for many of the symmetric [O I] profiles shown in the left panel, a few asymmetric profiles (90B, 07uy, and 08bo; *middle grouping*) exhibit emission peaks separated by $\sim 3000 \text{ km s}^{-1}$, i.e., close to

4.6. The Persistence of Blueshifted Emission Peaks

An important caveat to Figures 6 and 7 is that the [O I] $\lambda\lambda 6300, 6364$ profiles are snapshots of emission profiles at single epochs and thereby do not address possible evolutionary changes. From the handful of examples having multi-epoch observations, symmetric profiles show blueshifted emission peaks that slowly weaken in strength relative to their redshifted companions. For example, SN 2008ax, (Figure 2), SN 2004ao (Modjaz et al. 2007), and SN 2006T (compare day 106 of Modjaz et al. 2008a with day 371 of Taubenberger et al. 2009) all exhibit slow but measurable evolution in their double-peaked [O I] $\lambda\lambda 6300, 6364$ line profiles. Notably, the emission peaks maintain their blueshifted/redshifted velocities in all cases.

Asymmetric profiles, on the other hand, show a variety of evolutionary timescales in their emission peaks. As demonstrated by the persistent blueshifted peaks of SN 2004dk and SN 2005bf in Figure 6, and recent observations of SN 2008D observed on day 363 that show little change from day 91 (Modjaz et al. 2008b; Tanaka et al. 2009), some asymmetric profiles exhibit blueshifted peaks lasting hundreds of days. However, emission profiles like those seen in SN 2007uy and SN 2008bo are examples of asymmetric [O I] $\lambda\lambda 6300, 6364$ line profiles exhibiting blueshifted emission peaks

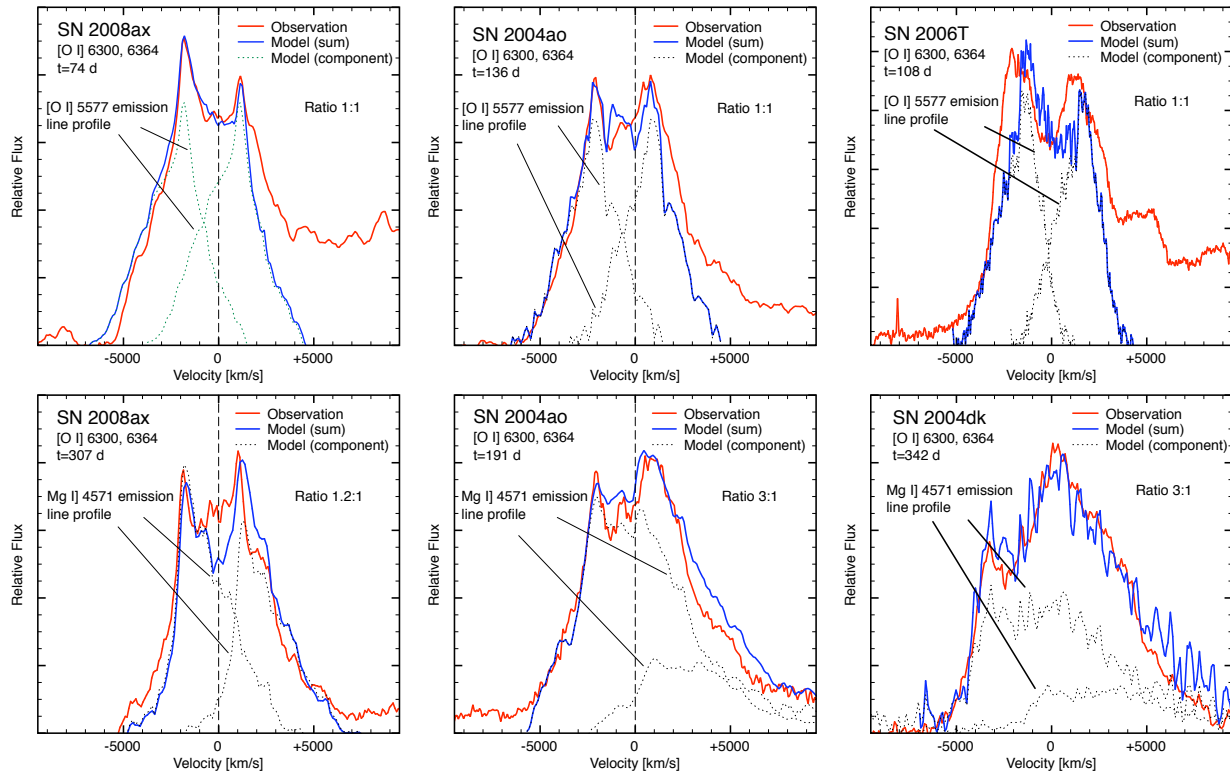


FIG. 8.— Model 1 for late-time [O I] $\lambda\lambda 6300, 6364$ emission: a single preferentially blueshifted emission component. Top panels are modeled with [O I] $\lambda\lambda 6300, 6364$ templates, bottom panels with Mg I $\lambda 4571$ templates. Observational data for SN 2004ao, 2004dk, and 2006T are from Modjaz et al. (2008a).

strength relative to emission near zero velocity tends to weaken.

5. THE NATURE OF [O I] $\lambda\lambda 6300, 6364$ LINE PROFILES

5.1. A Torus-like Distribution of O-rich Ejecta?

Several authors have proposed that double-peaked [O I] $\lambda\lambda 6300, 6364$ emission-line profiles are consistent with emission originating from a torus or disk of O-rich material, possibly orientated perpendicular to a rapidly expanding jet (Maeda et al. 2002; Mazzali et al. 2005; Maeda et al. 2006, 2008; Modjaz et al. 2008a; Tanaka et al. 2009). In this model, an object’s double-peaked [O I] profile reflects the observer’s fortunate orientation close to the plane of an expanding torus/disk of O-rich ejecta leading to blueshifted and redshifted emission peaks associated with the approaching and receding portions. Alternatively, viewing the torus perpendicular to the plane of expansion would result in a sharp, single-peaked [O I] line profile.

Some of the observational trends noted above in Section 4, however, signal warnings about adopting a

Double emission peaks seen in asymmetric profiles with separations larger or smaller than the doublet spacing (e.g., SN 2004dk and 2005bf) do not share this problem. However, the preferentially blueshifted emission profiles of Figure 6 illustrate the point that asymmetric profiles rarely show prominent peaks at wavelengths significantly longward of 6300 \AA . If the two observed emission peaks are attributed solely to the 6300 \AA line of [O I] originating from a toroidal geometry of ejecta, then one must interpret the tori to have centers of expansion having velocities blueshifted toward the observer, with the most redshifted portion of the expanding ring/torus at a velocity close to zero.

An example of a double-peaked [O I] $\lambda\lambda 6300, 6364$ profile interpreted this way was SN 2005bf (refer to Figure 6). Maeda et al. (2007) modeled the blueshifted profile as emission originating from a layered blob of Fe,Ca,O material either (1) unipolar and moving at a center-of-mass velocity $v \sim 2000 - 5000 \text{ km s}^{-1}$, or (2) suffering from self-absorption within the ejecta. In this case, the blueshifted double-peaked [O I] $\lambda\lambda 6300, 6364$ line profile was thought to be unique, and thus explanation (1) in-

5.2. Other Models

Complications with a torus/disk model raised by our observations prompted us to investigate two alternative interpretations of the double-peaked [O I] $\lambda\lambda 6300, 6364$ emission-line profiles. In light of mounting evidence that CCSNe are intrinsically aspherical, a torus geometry might still be correct but with considerable internal extinction. In cases like SN 2003jd where the expansion velocity is especially high and extinction is minimal, one may be truly seeing both blue and red sides of a shell or torus (Mazzali et al. 2005). However, in other cases where velocities are smaller and extinction is higher, the rear side of the ejecta and its emission might be hidden, even at epochs $t > 200$ d.

On the other hand, different line profiles observed in the oxygen and magnesium lines noted in Section 4 may originate from different regions of the SN. Line formation differences attributable to density, temperature, and energy potential dependencies may be introducing pronounced emission discrepancies between elements and species. Hence, the blueshifted, narrow profiles observed in [O I] $\lambda 5577$ and the zero velocity, broad profiles observed in O I $\lambda 7774$ may originate from two different regions of the SN: (1) a central, pseudo-spherically symmetric distribution of O-rich ejecta, and (2) a clump or shell of O-rich material traveling at a moderate velocity (-2000 to -4000 km s $^{-1}$) in the front-facing hemisphere.

We explored both of these scenarios in simple line fitting models. Below, we briefly discuss the results of these models, comment on their interpretations, and highlight their own associated difficulties.

5.2.1. A Single Blueshifted Emission Component?

The [O I] $\lambda\lambda 6300, 6364$ emission-line profile that would follow from a single preferentially blueshifted emission source was investigated first. This configuration mimics emission originating from a blueshifted, optically thick, and high density region (possibly the front side of a ring, torus, or hollow shell with densities upward of 10^{10} cm $^{-3}$) where the 6300:6364 flux ratio could approach unity and the lack of a corresponding redshifted emission peak might be due to significant internal extinction in the ejecta.

Both observed [O I] $\lambda 5577$ and Mg I] $\lambda 4571$ emission-line profiles were used as templates for the [O I] $\lambda\lambda 6300, 6364$ lines. The [O I] $\lambda 5577$ profiles were used for earlier epochs ($t \lesssim 100$ d) and the Mg I] $\lambda 4571$ at later ones ($t \gtrsim 200$ d), as these epochs represent when the lines are best observed. The template profiles were separated by 3000 km s $^{-1}$ in velocity, added, and the result scaled to match the amplitude of the observed [O I] $\lambda\lambda 6300, 6364$ profile of the same epoch. The SNe having the best time

contribution from other lines to the red of the oxygen emission as evidenced by the moderate strength emission at higher redward velocities. The agreement is good for SN 2008ax and 2004ao, but rather poor in SN 2006T where peak height is adequately matched but position and width is not.

The bottom panels of Figure 8 present [O I] line models using the Mg I] $\lambda 4571$ line template. Both SN 2004ao and 2004dk show good agreement and were best fit with templates added in a 3:1 ratio. However, SN 2008ax was best fit with a ratio of 1.2:1.0 and showed an overall reasonable fit but with noticeable disparity between the line model and observation around zero velocity.

The results with our single component line fitting models corroborate observations made in the Taubenberger et al. (2009) survey of [O I] $\lambda\lambda 6300, 6364$ profiles of Ib/c SN. Taubenberger et al. also used emission-line profiles of Mg I] $\lambda 4571$ to model [O I] $\lambda\lambda 6300, 6364$ profiles as we have done here, and found general agreement between the two profiles at sufficiently late phases. Furthermore, among the double-peaked profiles they modeled, Taubenberger et al. reported that two SNe, SN 2000ew and 2004gt, could be fit very well with Gaussian distributions of the deblended $\lambda\lambda 6300, 6364$ lines originating from a single narrow, blueshifted component.

Although the one-component line fitting models are encouraging in five out of six profiles presented here, attributing double-peaked [O I] emission to the two doublet lines has problems. The most serious problem is the origin of the preferentially blueshifted emission. Expansion of SN ejecta should lower density significantly such that emitted optical photons have minimal interaction with the gas at nebular epochs (Maeda et al. 2008), but the $\sim 1:1$ flux ratio of the SN 2004ao and 2008ax [O I] $\lambda\lambda 6300, 6364$ line models and the lack of redshifted emission imply a significantly high optical depth even at epochs of day ~ 100 and greater.

Another potential problem for the single component model is the evolution of the blue/red peak height ratio. As seen in Figure 2, the blueshifted peak decreases in strength relative to the redshifted peak with time. The opposite evolution is expected, however, if the two peaks are associated with the [O I] $\lambda\lambda 6300, 6364$ doublet lines, since expansion of the SN should drive the blue/red peak height ratio towards the nebular 3:1 ratio. A similar blue/red peak evolution away from the nebular 3:1 ratio in the [O I] $\lambda\lambda 6300, 6364$ profile of SN 2004ao led Modjaz et al. (2008a) to conclude that the doublet lines were likely not behind the observed emission peaks.

However, the evolution of the [O I] 5577 line profile in SN 2008ax offers a possible explanation of the ratio change observed between emission peaks. Our multi-

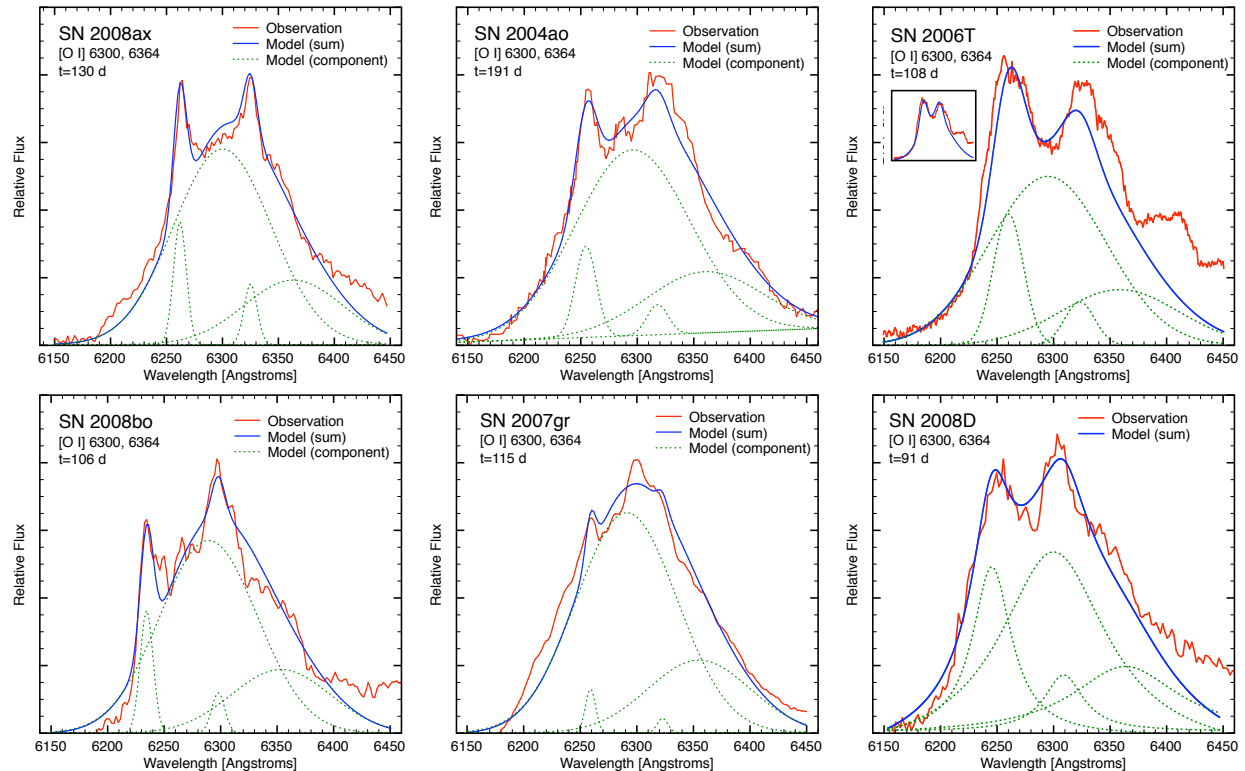


FIG. 9.— Model 2 for late-time [O I] $\lambda\lambda 6300, 6364$ emission: broad emission centered around zero velocity with a narrow blueshifted emission component. *Top*: symmetric profiles. *Bottom*: asymmetric profiles. Observational data for SN 2004ao are from Modjaz et al. (2008a). All line models adopt an [O I] 6300:6364 flux ratio of 3:1, except for the inset of SN 2006T where a ratio of 1.8:1 was used.

5.2.2. Broad Emission Plus a Blueshifted Emission Component?

We next investigated the [O I] $\lambda\lambda 6300, 6364$ line profile that would follow from the contribution of two emission components. Line fitting models of [O I] $\lambda\lambda 6300, 6364$ emissions were constructed using the IRAF package SPECFIT (Kriss 1994). Each profile fit consisted of five sources: (1) a linear continuum, (2) a *broad* (FWHM ~ 6000 km s $^{-1}$) Gaussian centered at 6300 ± 10 Å, (3) another Gaussian shifted 64 Å to the red fixed with the same FWHM but one third its strength, (4) a *narrow* (FWHM ~ 1000 km s $^{-1}$) Gaussian at a blueshifted wavelength, and (5) another narrow Gaussian 64 Å to the red fixed with the same FWHM and one third its strength. The free parameters were the strength of the linear continuum, and the position, FWHMs, and relative strengths of the pairs of peaks. The line profile model was tested with four SNe (SN 2007gr, SN 2008ax, SN 2008bo, and SN 2004ao from Modjaz et al. 2008a) showing symmetric and asymmetric profiles.

In Figure 9 we present the results of these recon-

agreement in the peak separation and individual width was evident.

The bottom panels of Figure 9 present our line fitting results for asymmetric profiles. In all cases the agreement is good, although agreement is relatively poor in SN 2007gr near the zero velocity peak. This discrepancy, as well as discrepancies in other line models, may in part be a reflection of the inadequate use of Gaussian distributions to model the emission.

The fixed 3:1 ratio used for the two components would seem to run counter to the evolution of the blue/red peak height ratio observed in symmetric profiles. However, Taubenberger et al. (2009) recently concluded that the line centroids of the bulk of [O I] emission at phases earlier than day ~ 200 were blueshifted ~ 20 Å, after which they drift close to zero velocity. This phenomenon offers an explanation for the apparent 6300:6364 ratio decrease over observed epochs. Assuming a broad/central + narrow/blueshifted interpretation, a gradual shift toward zero velocity of the broad component would cause the blueshifted $\lambda 6300$ line of the narrow component to weaken in strength relative to the $\lambda 6364$ companion line.

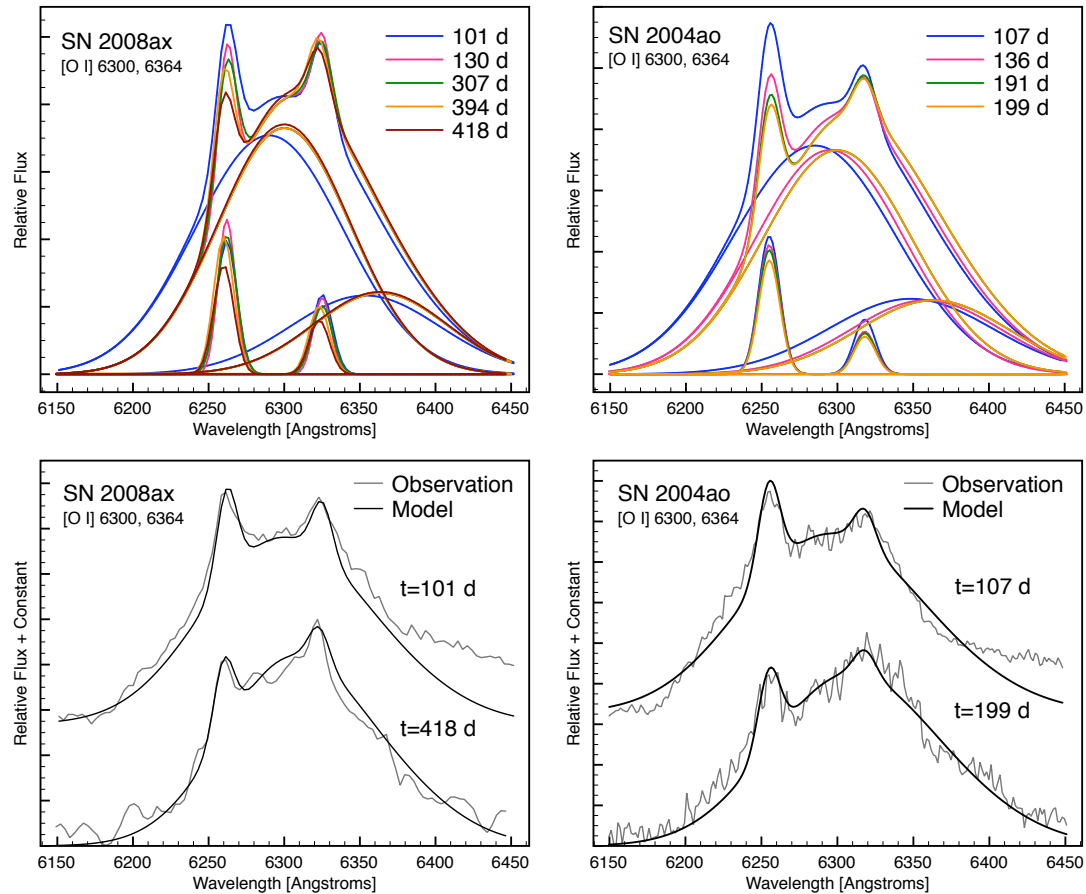


FIG. 10.— Line fitting models for the evolution of two symmetric profiles following the decline of blueshifted emission peaks using the two-component model illustrated in Figure 9. Variables changed between epochs are relative strength between narrow and broad components and the central wavelength of the broad distribution. [O I] 6300:6364 flux ratios of $\approx 2:1$ and $3:1$ were adopted for SN 2008ax and SN 2004ao, respectively. Slight changes to the FWHMs of the distributions are introduced to compensate for changes in spectral resolution. Broad distributions originally blueshifted $\sim 20 \text{ \AA}$ at $t \sim 100 \text{ d}$ gradually shift towards zero velocity by 200 d and the narrow blueshifted components weaken in relative strength. Top panels show models for all epochs, and bottom panels compare models and observed data for first and last epochs. Observational data for SN 2004ao are from Modjaz et al. (2008a).

tions introduces considerable uncertainty in the veracity of the model fits.

Aside from these modeling concerns, there is also the question of why clumps are mainly visible on the forward facing hemisphere, and rarely from the rear side. If clumps were randomly distributed, a variety of blueshifted and redshifted emission peaks would be expected. Any explanation in which a preferential visibility of blueshifted peaks might be caused by high internal extinction is complicated by the fact that considerable broad emission is seen at both higher blueshifted and redshifted velocities.

6. DISCUSSION AND CONCLUSIONS

sharp, and well defined [O I] emission peaks, we used SN 2008ax to help guide the investigation. We also examined the late-time [O I] $\lambda\lambda 6300, 6364$ line profiles of 13 other stripped-envelope CCSNe taken from the literature.

6.1. Empirical Results of Our Study

Our investigation into the properties of late-time [O I] $\lambda\lambda 6300, 6364$ line profiles of stripped CCSNe exhibiting double-peaked line profiles showed the following:

- Doubled-peaked line profiles are primarily in [O I] $\lambda\lambda 6300, 6364$ emission (Figure 4 and 5) and can be categorized into two types. One type shows conspicuous symmetric emission peaks positioned about 6300 \AA that

are simply reflecting the doublet nature of the [O I] line emission. Over time, the velocities of the two peaks do not change, but the blue/red peak intensity ratio slowly decreases.

- Conspicuous redshifted emission peaks are not observed in asymmetric profile cases. As seen for symmetric profiles, the position of blueshifted peaks does not change between observed epochs, but their strength relative to emission near zero velocity tends to weaken with time.

- When double-peaked [O I] profiles are present, single-peaked emission peaks at blueshifted velocities matching blueshifted peaks in [O I] $\lambda\lambda 6300, 6364$ are often seen for [O I] $\lambda 5577$. The Mg I $\lambda 4571$ and O I $\lambda 7774$ lines generally show more blueshifted emission than redshifted emission and sometimes evidence of peaks at velocities matching blueshifted and/or zero-velocity peaks in the [O I] $\lambda\lambda 6300, 6364$ lines.

6.2. Results of Double-peaked [O I] Line Profiles Fits

The high incidence of $\approx 64 \text{ \AA}$ separation between emission peaks of symmetric profiles plus the lack of redshifted emission peaks in asymmetric profiles suggests that emission from the rear of the SN may be suppressed. This leads us to conclude that double-peaked [O I] $\lambda\lambda 6300, 6364$ line profiles of some stripped-envelope, core-collapse SNe are not necessarily signatures of emission from the front and rear faces of a torus or elongated shell of O-rich ejecta as has been proposed.

Alternative interpretations for the observed [O I] $\lambda\lambda 6300, 6364$ profiles were investigated through line-fitting models. Two models were explored: Model 1 where the [O I] profile arises only from preferentially blueshifted emission, and Model 2 where the [O I] profile consists of two separate emission components, a broad emission source centered around zero velocity and a narrow, blueshifted source. Both line-fitting models reproduced observed [O I] $\lambda\lambda 6300, 6364$ profiles in the majority of test cases. Model 2 showed better overall agreement to the data for all six cases of symmetric and asymmetric profiles across all epochs investigated, but Model 1 had fewer parameters and convincing results in a subset of the symmetric profiles. Similar line-fitting results have been reported in Taubenberger et al. (2009).

It should be noted that a torus or elongated shell model is still viable despite the concerns raised above if the rear portion of an O-rich torus or shell is somehow hidden by scattering or dust. Moreover, two of the 18 SNe studied in this sample, SN 2003jd and 2006T, exhibited both blueshifted and redshifted emission peaks with separations and widths that could not be modeled under the

Why do these emission-line profiles lack redshifted emission peaks? The predominance of blueshifted emission features in the profiles studied is unclear but internal scattering or dust obscuration of emission from far side ejecta are the most likely scenarios. Taubenberger et al. (2009), who also found predominantly blueshifted peaks in [O I] $\lambda\lambda 6300, 6364$ emission-line profiles in a sample of 39 Type Ib/c SNe, favored an opaque inner ejecta scenario, citing that other explanations such as ejecta geometry, dust formation, and contamination from other lines, could not account for all observed trends.

What is the physical nature of these blueshifted features? The variety and strength of the emission peaks are suggestive of asphericity in the ejecta. But whether these features can be conclusively associated with cones, jets, or tori of unipolar/bipolar explosions is uncertain and beyond the scope of this paper. We note that the difference between symmetric and asymmetric profiles in our two-component line-fitting models is a consequence of the parameters adopted for the narrow, blueshifted component (i.e., FWHM, central velocity, strength relative to the broad component near zero velocity, and 6300:6364 flux ratio). Sophisticated models incorporating radiative transfer effects could explore how these line-fitting parameters may be related to physical quantities such as mass, velocity, size, and density of the O-rich material, as well as changes with viewing angle. Such models could also investigate specific extinction mechanisms of the suspected opaque inner region.

6.4. Future Observations

Much more robust tests of line-fitting models are possible with spectra of improved time coverage, spectral resolution, and S/N for those CCSNe displaying double-peaked [O I] $\lambda\lambda 6300, 6364$ profiles. Moreover, observations optimized around the lines of Mg I $\lambda 4571$, [O I] $\lambda 5577$, and O I $\lambda 7774$ at late epochs starting from 50 days past maximum light could greatly help test the trends observed in our sample and help eliminate one of the two line models (single or two component) discussed here. Infrared observations might also place constraints on the cause of the suspected internal extinction. While an opaque inner region appears to best explain the lack of redshifted features, late-time infrared studies of other stripped-envelope CCSNe could characterize the presence of internal molecules and dust as a test of one source of extinction at the epochs studied here.

This work has made use of data from many previous observers which proved invaluable in our analysis. We thank M. Modjaz for many helpful comments and kindly providing spectra for SN 2004ao, SN 2006T, SN 2005bf, SN 2004bl, SN 2004F, and SN 2002D. We thank the

REFERENCES

- Blondin, S., & Calkins, M. 2008, CBE Tel., 1191, 2
 Blondin, S., & Tonry, J. L. 2007, ApJ, 666, 1024
 Chornock, R., et al. 2007, CBE Tel., 1036, 1
 Chornock, R., et al. 2008, CBE Tel., 1298, 1
 Clocchiatti, A., et al. 2001, ApJ, 553, 886
 Crockett, R. M., et al. 2008a, ApJ, 672, L99
 Crockett, R. M., et al. 2008b, MNRAS, 391, L5
 Fabricant, D., Cheimets, P., Caldwell, N., & Geary, J. 1998, PASP, 110, 79
 Filippenko, A. V. 1997, ARA&A, 35, 309
 Filippenko, A. V., Matheson, T., & Barth, A. J. 1994, AJ, 108, 2220
 Fransson, C., & Chevalier, R. A. 1989, ApJ, 343, 323
 Houck, J. C., & Fransson, C., 1996, ApJ, 456, 811
 Hungerford, A. L., Fryer, C. L., & Rockefeller, G. 2005, ApJ, 635, 487
 Hunter, D., J., et al. 2009, A&A, 508, 371
 Kriss, G., 1994, in ASP Conf. Ser. 61, Astronomical Data Analysis Software and Systems III, ed. D. R. Crabtree, R. J. Hanisch, & J. Barnes (San Francisco: ASP), 437
 Leonard, D. C., Filippenko, A. V., Chornock, R., & Foley, R. J. 2002, PASP, 114, 1333
 Li, H., & McCray, R. 1992, ApJ, 387, 309
 Madison, D., & Li, W. 2007, CBE Tel., 1034, 1
 Maeda, K., et al. 2008, Science, 319, 1220
 Maeda, K., et al. 2007, ApJ, 666, 1069
 Maeda, K., Nomoto, K., Mazzali, P. A., & Deng, J. 2006, ApJ, 640, 854
 Maeda, K., et al. 2002, ApJ, 565, 405
 Matheson, T., et al. 2008, AJ, 135, 1598
 Matheson, T., Filippenko, A. V., Li, W., Douglas, L. C., Shields, J. C. 2001, AJ, 121, 1648
 Matheson, T. M., et al. 2000a, AJ, 120, 1487
 Matheson, T. M., Filippenko, A. V., Ho, L. C., Barth, A. J., & Leonard, D. C. 2000b, AJ, 120, 1499
 Mazzali, P. A., et al. 2007, ApJ, 670, 592
 Mazzali, P. A., et al. 2005, Science, 308, 1284
 Mazzali, P. A., et al. 2002, ApJ, 572, 61
 Modjaz, M., Kirshner, R. P., Blondin, S., Challis, P., & Matheson, T. 2008a, ApJ, 687, L9
 Modjaz, M., et al. 2008b, ApJ, 702, 226
 Modjaz, M. 2007, Ph.D. thesis, Harvard Univ.
 Morrell, N., Folatelli, G., & Stritzinger, M. 2007, CBE Tel., 1160, 1
 Mostardi, R., Li, W., & Filippenko, A. V. 2008, CBE Tel., 1280, 1
 Nakano, S., Kadota, K., Itagaki, K., Corelli, P. 2008, IAU Circ. 8908, 2
 Navasardyan, H., et al. 2008, CBE Tel., 1325, 1
 Nissinen, M., & Oksanen, A. 2008, CBE Tel., 1324, 1
 Parisky, X., & Li, W. 2007, CBE Tel., 1158
 Pastorello, A., et al. 2008, MNRAS, 389, 955
 Qiu, Y., Li, W., Qiao, Q., & Hu, J. 1999, AJ, 117, 736
 Schmidt, G., Weyman, R., & Foltz, C. 1989, PASP, 101, 713
 Sollerman, J., Leibundgut, B., & Spyromilio, J. 1998, A&A, 337, 207
 Spyromilio, J. 1994, MNRAS, 266, L61
 Spyromilio, J. 1991, MNRAS, 253, 25
 Spyromilio, J., et al. 1991, MNRAS, 248, 465
 Tanaka, M., et al. 2009, ApJ, 700, 1680
 Taubenberger, S., et al. 2009, MNRAS, 397, 677
 Valenti, S., et al. 2008a, ApJ, 673, L155
 Valenti, S., et al. 2008b, MNRAS, 383, 1485
 Wang, L., & Hu, J. Y. 1994, Nature, 369, 380
 Williams, R. E. 1994, ApJ, 426, 279